Available online at www.sciencedirect.com
SCIENCE DIRECT®
Journal of Solid State Chemistry 178 (2005) 1376–1385
JOURNAL OF SOLID STATE CHEMISTRY
www.elsevier.com/locate/jssc

The ordered phase of methylammonium lead chloride $CH_3ND_3PbCl_3$

Lisheng Chi[a,*], Ian Swainson[a], Lachlan Cranswick[a], Jae-Hyuk Her[b], Peter Stephens[b], Osvald Knop[c]

[a]*Chalk River Laboratories, National Research Council of Canada, Neutron Program for Materials Research, Steacie Institute for Molecular Sciences, Building 459, Station 18, Chalk River Laboratories, ON, Canada K0J 1J0*
[b]*Department of Physics & Astronomy, State University of New York, Stony Brook, NY 11794-3800, USA*
[c]*Department of Chemistry, Dalhousie University, Halifax, NS, Canada B3H 4J3*

Received 2 November 2004; received in revised form 8 December 2004; accepted 17 December 2004
Available online 16 March 2005

Abstract

The perovskite-structured compound methylammonium lead chloride orders into a low-temperature phase of space group *Pnma*, in which at 80 K each of the orthorhombic axes $a = 11.1747(2)$ Å, $b = 11.3552(1)$ Å and $c = 11.2820(1)$ Å is doubled with respect to the room temperature disordered cubic phase ($a = 5.669$ Å). The structure was solved by ab initio methods using the programs EXPO and FOX. This unusual cell basis for space group *Pnma* is not that of a standard tilt system. This phase, in which the methylammonium ions, are ordered shows distorted octahedra. The octahedra possess a bond angle variance of $60.663^{\circ 2}$ and a quadratic elongation of 1.018, and are more distorted than those in the ordered phase of methylammonium lead bromide. There is also an alternating long and short Pb–Cl bond along *a*, due to an off-center displacement of Pb within the octahedron. This suggests that the most rigid unit is actually the methylammonium cation, rather than the $PbCl_6$ octahedra, in agreement with existing spectroscopic data.

Keywords: Perovskite; Methylammonium lead chloride; Phase transition; Neutron and synchrotron powder diffraction; Rietveld refinement

1. Introduction

The perovskites, usually written as ABX_3, comprise a set of fully corner-sharing $BX_{6/2}$ octahedra creating a three-dimensional framework, and are a well-studied system of crystal structures, both in terms of the underlying physics of their phase transitions and their crystal chemistry. The *A* site is usually occupied by a simple cation for charge balancing, although it may also be vacant, as in the bronze compounds such as WO_3, where charge balancing is not required. Mitchell has recently given a review of the great variety of perovskites and related phases [1].

There is another class of true perovskites in which *A* is a molecular cation. Various amines may be placed on the *A*-site, such as ammonium NH_4^+ [2], methylammonium $CH_3NH_3^+$ [3–6], and formamidinium $NH_2CH{=}NH_2^+$ [7,8]. These are particularly common in compounds based around lead and tin halides. In the cubic phase, the site symmetry of the *A* cation $m\bar{3}m$ exceeds the molecular symmetry of these amines, and they must therefore be disordered. Order–disorder behavior of the cations is intrinsically coupled to distortions of the perovskite framework.

This class of perovskite holds an interesting place in the study of order–disorder phenomena in molecular solids. For true molecular crystals displaying order–disorder transitions, such as SF_6 and CBr_4 [9], direct displacive and orientational interactions between molecules occur. These order–disorder transitions are typically driven by soft modes, which are external modes of these molecules, low-lying in frequency, and typically well separated in energy from the internal modes. For

*Corresponding author. Fax: +1 613 584 4040.
E-mail address: Lisheng.Chi@nrc.gc.ca (L. Chi).

0022-4596/$ - see front matter Crown Copyright © 2005 Published by Elsevier Inc. All rights reserved.
doi:10.1016/j.jssc.2004.12.037

framework structures, such as perovskites, consisting of concatenated molecular units, there is a small set of external modes of the molecular units, termed Rigid Unit Modes (RUMs) that are consistent with the connectivity of the framework. These occur due to a small excess of degrees of freedom with respect to the number of geometrical constraints in the structure [10,11].

The corner-bonded nature of the perovskites therefore generates a set of transitions, which have become known as the tilt transitions. These were first classified by examination in real space by Glazer [12,13]. Both the RUM-phonon approach [10,11] and the group theory approach of Howard and Stokes [14] use the constraint of undistorted octahedra undergoing tilting as an approximation in their calculations. Distortions of these octahedra may occur in the resulting subgroups, but the key point is that such distortions are not generally required. These approaches ignore the *A* cations, which are "passive" in the sense that the presence or absence of a given cation does not generate any new possible tilt transitions, but may stabilize the choice of a given tilt system.

In the case of the methylammonium lead halides ($MAPbX_3$), there are both molecular cations and anions. Both of these entities can be considered to have their own external modes. As the anions are totally corner-bonded, clearly the anions possess strong direct interactions between one another. However cation–cation interactions will be mainly indirect, as they are isolated from one another in the perovskite cages. So while the analogous Cs-perovskites, $CsPbCl_3$ and $CsPbBr_3$ show tilt transitions [15,16], one might therefore expect that the loss of symmetry through ordering phase transitions in $MAPbX_3$ would be favorably described through rotations and, possibly, distortions of the network of anion octahedra. In this work, we will show that orientational ordering of the methylammonium units and the hydrogen bonding between methylammonium and chloride ions significantly distorts the network of octahedra.

The methylammonium Sn(II)-halide perovskite system and the large variety of related layered perovskites, which form with longer chained amines [7,17,18], as well as Ge(II) analogues [19,20], have been extensively studied, in part due to their interesting electrical properties. The behavior of formamidinium tin iodide under pressure has been interpreted in terms of tilting of rigid octahedra [8]. High electric conductivity has been observed in $CH_3NH_3GeCl_3$ above 398 K [20]. Less attention has been paid to the Pb-based perovskites. Poglitsch and Weber performed the first study of the ordered space groups of $MAPbX_3$ (X = Cl, Br, I) and deduced space groups of the ordered states on the basis of observed systematic absences from low-temperature Guinier data [4]. They detected three phases at ambient pressure: the cubic $Pm\bar{3}m$ Phase I at room temperature, a quasi-tetragonal Phase II having a limited stability field of a few degrees, and an orthorhombic Phase III below about 172 K [4]. They suggested that the ordered states of $MAPbX_3$ are all non-centrosymmetric and are therefore possible ferroelectrics, which is a possibility consistent with the permanent dipole of the MA cation. They proposed the space group of the low temperature phase of $MAPbCl_3$ was $P222_1$, and that the cell sides were $a = 5.67$ Å, $b = 5.63$ Å, $c = 11.18$ Å; i.e., doubled only along c with respect to the cubic form. (However, although this is non-centrosymmetric, it is not a polar group and therefore could not display ferroelectricity.) Of the $MAPbX_3$ system, $MAPbCl_3$ is probably the most intensely studied, including by NMR [5,21], Raman studies [22–24], calorimetry [5,25] and pseudo-spin descriptions of the phase transition [26].

A single crystal diffraction pattern of Phase II of $MAPbCl_3$ was presented by Kawamura and Mashiyama [27], who observed both superlattice and incommensurate satellite reflections in an oscillation photograph taken about 0 0 *l*. The Miller indexes of these reflections were respectively assigned as (odd/2, 4, 0) and (integer/3, 4, 0). They determined the lattice parameters to be $a = 11.274$ Å, $b = 11.354$ Å and $c = 11.208$ Å. They suggested it plausible that Phase III was orthorhombic and that $P2_12_12_1$, was the space group, although their crystal was twinned.

Until recently, there has been little questioning of the space groups proposed by Poglitsch and Weber [4] for the ordered phases of $MAPbX_3$. Although group theory [14] limits the symmetries possible for tilt transitions for the true perovskites with simple or no *A* cations, one might expect unusual symmetries to be produced as the dipoles of the MA cations order in the cages. The present experiment is motivated by an interest in studying this possibility.

2. Experimental

2.1. Sample preparation

Samples were prepared according to the description of Refs. [3,5]. In order to N-deuterate samples, the exchangeable protons of the precursors, CH_3NH_3Cl and lead acetate, were replaced by solution in D_2O, as described in Ref. [6]. Deuterated CH_3ND_3Cl and Pb acetate were dissolved in excess of hot DCl solution. The mole ratio of CH_3ND_3Cl and Pb acetate is at least 8 to obtain pure product. Methylammonium chloride solution was slowly added into Pb acetate solution drop-by-drop while heating and stirring. A light-yellow solid was precipitated. After the solution cooled down, the solid was filtered and washed in benzene and then dried. N-deuterated samples reduce the incoherent scattering

to reasonable levels, and isotopically label the amine end of the MA cation with positive scattering D, and the methyl end with negatively scattering H.

2.2. Data collection

The synchrotron X-ray powder diffraction pattern was collected on the X3B1 beamline at the National Synchrotron Light Source, Brookhaven National Laboratory. X-rays of wavelength 0.69944(1) Å were selected with a Si(111) double crystal monochromator; after the sample, the diffracted beam was analyzed by a Ge(111) crystal and detected by a NaI scintillation counter. This configuration gives angular resolution on the order of 0.007–0.02° full width at half maximum. Wavelength and diffractometer zero were calibrated by measuring a sample of NIST Standard Reference Material 1976 (sintered plate of Al_2O_3). The powder sample was mounted on a flat brass plate, 15 mm wide along the incident beam direction, and oscillated by 5° about the dividing position during data acquisition. The sample was mounted in a closed-cycle He cryostat, regulated at 80 K.

The neutron powder diffraction measurements were performed on the C2 neutron powder diffractometer at the NRU reactor, Chalk River, Ontario. This consists of an 800-wire BF_3 detector, which floats over an epoxy dancefloor with the aid of a high-pressure air supply. The wavelength of the runs was calibrated as 1.3276(2) Å with an external standard of NIST Si 640c. The powder sample was hand ground in a pestle and mortar and transferred to a vanadium can of 5 mm diameter. The temperature was controlled with a top-loading, three-stage cold-cycle refrigerator manufactured by Janis, with a Sumitomo Heavy Industries 950-T compressor. This is capable of control between 3.5 K and room temperature. Temperatures were controlled using a DT670B sensor, and sample temperatures were read with Cernox sensors at either end of the cylindrical can. All gradients were less than 0.1 K. The data were collected up to $2\theta = 84.9°$ with $\Delta(2\theta) = 0.1°$.

2.3. Indexing, model generation and refinement methods

High resolution X-ray diffraction data were important to establish the systematic absences needed to determine the correct space group, relative to previous published work [4,27]. The synchrotron data from Phase III were indexed using the Crysfire suite of software [28], generating an orthorhombic cell of approximately 11.17, 11.36 and 11.28 Å, which is related to the cubic cell by doubling along all cubic cell edges, a_P; i.e. $(2a_P \times 2a_P \times 2a_P)$. From the systematic absences observed in the synchrotron powder data, the most likely space group was *Pnma*. We make particular note that this is not the standard *Pnma* cell found in tilted perovskites which possesses the basis $\sqrt{2}a_P \times 2a_P \times \sqrt{2}a_P$. The basis $2a_P \times 2a_P \times 2a_P$ is usually associated with *Cmcm* in tilted perovskites, but this is not possible in this case as there are clear C-centering violations, which are quite strong in the neutron data, but also visible as weak superlattices in the synchrotron data. This is shown in Fig. 1 where the overlapped peaks from (101) and (011), both C-violations, are shown at ~9.5° 2θ in the neutron data.

As a *Pnma* cell with this basis is not a common perovskite cell, it was not immediately apparent on which sites the octahedra and MA cations sat. The MA cation has $3m$ molecular symmetry. Any ordered phase of a MA-based perovskite therefore must leave the MA ion sitting on a crystallographic site compatible with the molecular symmetry; i.e., the site must be of symmetry $3m$, 3, m, or 1. Sites with symmetry m and 1 exist in *Pnma*.

The direct methods package EXPO [29] was used on the synchrotron data to find on which sites the octahedra sat in the *Pnma* cell. Preliminary refinements with the octahedra on various sites in the unit cell were attempted for comparison. The best fits were found with the octahedra on the general equivalent positions, and the MA ions on mirrors. In another approach, we used the ab initio direct space program FOX [30] to optimize structural models with respect to both the neutron and synchrotron data. This program is capable of trying all conceivable choices for placing the molecular anions and cations in the cell, removing excess copies of these entities when it places them on high symmetry sites, and merging atoms, when it discovers concatenation. For the FOX optimizations, we used models with highly flexible $PbCl_6$ octahedra, and soft bond length, bond angle and angle restraints for the MA cation, based on the refinements of $MAPbBr_3$ [6]. FOX chose the same positions for the octahedron and the MA ions in the *Pnma* cell, as had been determined by the earlier method. There are two symmetrically distinct sites for the MA cation in this structure.

Joint neutron and synchrotron refinements were performed using GSAS [31]. The synchrotron powder data were refined for $2\theta > 17.5°$, to reduce the effect of spill over of the beam from the flat plate sample at low angles. We note that the two lowest peaks, (011) and (101), are some of the strongest in the neutron pattern representing ordering of the MA ion in the Pb–Cl cage. These peaks were very weak in the synchrotron data, and could not be discerned in our preliminary laboratory X-ray studies that we had performed. The Rietveld profile fit is given in Fig. 1. Lattice parameters and agreement factors are listed in Table 1, indicating that the structure we have determined is a very good fit to the neutron and X-ray experimental data. Although there were no peaks from the synchrotron data that could not be explained from *Pnma*, as with the earlier work on

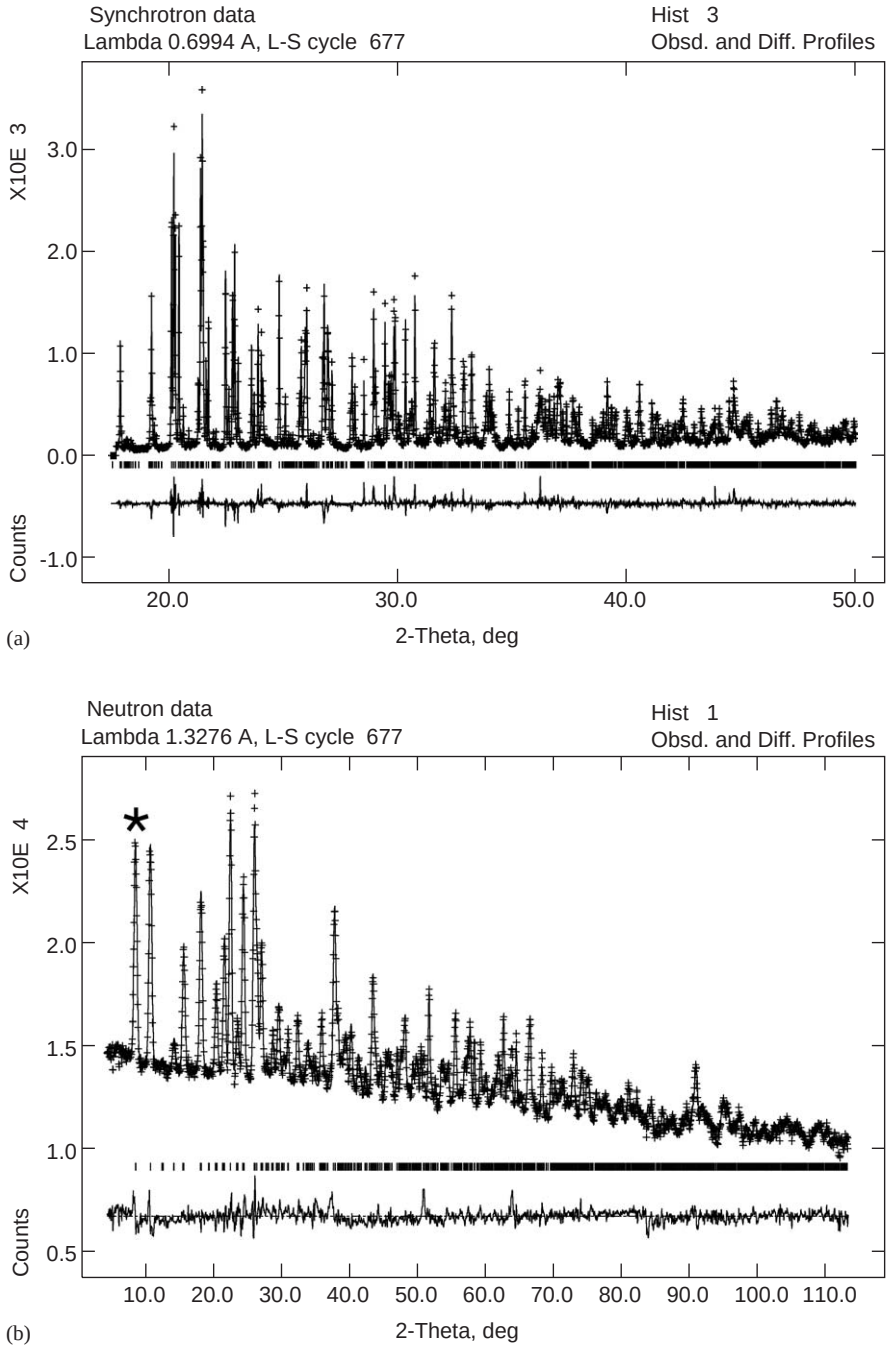

Fig. 1. Rietveld profile refinement for synchrotron (a) and neutron (b) powder patterns at 80 K. The dots are for observed data, solid line is the fit, vertical marks indicate Bragg peaks and bottle line is the difference intensity. The peak in the neutron pattern marked with * represents contributions from (011) to (101), both violating C-centering.

Table 1
Refined crystallographic parameters with combined neutron and synchrotron data in $MAPbCl_3$ at 80 K

Parameters	Neutron data	Synchrotron data	Total powder
χ^2	3.574		
R_{wp}	0.0212	0.0847	0.0257
R_p	0.0163	0.0667	0.0179
N_{obs}	1632	1411	

SG: *Pnma*; Lattice parameters: $a = 11.1747(2)$ Å, $b = 11.3552(1)$ Å, $c = 11.2820(1)$ Å.

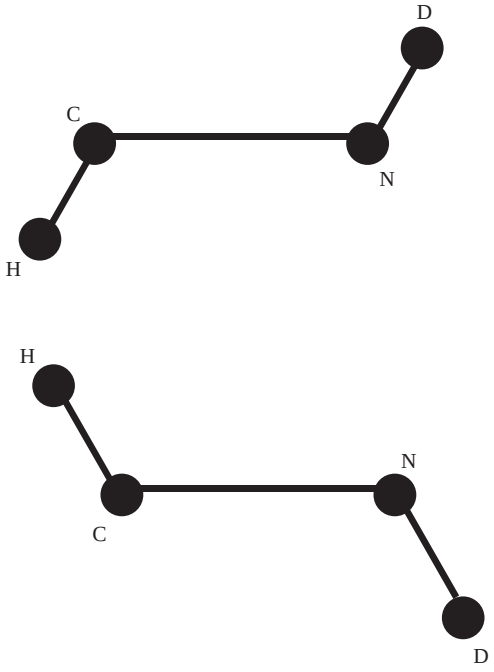

Fig. 2. Schematic of the two ways in which a methylammonium ion can lie in the mirror, lying in the plane of the paper. Only the bonds which lie on the mirror are shown. These cannot be rotated into one another within the mirror.

$MAPbBr_3$, we checked various subgroups of *Pnma,* including the non-centrosymmetric, but orthorhombic, $P2_12_12_1$, and the monoclinic subgroup $P2_1/m$. Tests on the output of these refinements using Platon/Addsym [32] confirmed the *Pnma* cell.

Neutrons provide the only rigorous method for determining the positions of light atoms, and there have been several examples, such as ammonium cyanate, where hydrogen-bonding systems have been incorrectly estimated from X-ray data, e.g. [33]. The MA cations occupy two inequivalent sites, and there are two inequivalent ways of placing an MA cation on the mirror in each (Fig. 2). A rigid body description, similar to that used in Ref. [6], of both choices (denoted type *A* and *B*) of the MA cation for both the MA sites was used in these refinements. This gives rise to four refinement models (AA, AB, BA and BB) to test. The model BB gave a significantly lower R_p for the neutron patterns than the others.

3. Results and discussion

The refined atomic coordinates and thermal parameters are given in Table 2, and selected bond lengths and angles in Table 3.

As was found for $MAPbBr_3$, the interatomic distances between the deuterons on the amine end and the chlorine atoms are shorter than the corresponding distances to the hydrogens on the methyl end for both MA ions (Table 3), as one would expect if hydrogen bonds were generated between the cation and the cage.

Fig. 3 presents a projection of the crystal structure of $MAPbCl_3$ viewed down the *b*-axis in which (Fig. 3(a)) MA ions are antiferro-ordered down the *b*-axis. While the cell is centrosymmetric, the octahedra do not lie on the center of symmetry: there is considerable internal distortion of the octahedra (Table 3). There is in particular an alternating long Pb–Cl bond 3.024(5) Å and short Pb–Cl bond 2.729(5) Å, sub-parallel to [100]. Fig. 3(b) displays the hydrogen–chlorine connectivity between the $PbCl_6$ octahedron and the MA ion. The alternating long and short Pb–Cl bond lengths are related to Pb-displacements, which may be a weak lone pair effect. We also note that the average bond length of 2.861 Å is longer than that extrapolated from the cubic phase ($a_p/2$). This is characteristic of dynamic disorder in high-symmetry framework structures [34,35].

Although the octahedron in $MAPbCl_3$ is considerably distorted, calculation of the octahedral tilting parameters on the basis of definition by Thomas [36] is still valuable in the quantitative analysis of octahedral tilting. We note that in this structure the stalk lengths, s_1 and s_2, represent Cl–Cl distances which do not necessarily intersect the Pb atom. Table 4 lists calculated tilting parameters, where θ_m is the mean tilting of θ_x and θ_y, which are angles between the *x*- and *y*-axis and the closest stalks, while θ_z is an angle between the *z*-axis and the nearest stalk. The function $\Phi = 1 - \cos^2\theta_m \cos\theta_z$ represents the total degree of tilting. The observed polyhedral volumes $V_{A,1}$, $V_{A,2,}$ and V_B were taken from calculations from IVTON [37]. The quadratic elongation and bond angle variance are from VOLCAL analysis in WINGX [38,39]. We note that the value of QE_B is greater than one, whereas $(s_1+s_2)^2/s_1s_2 = 4.000$, showing that much of the linear distortion of the octahedron is internal. The discrepancy between V_A/V_B^t and V_A/V_B^a represents deviation of the three octahedral stalks from normal intersection, another index for distortion of octahedra. This is reflected in the fact that $MAPbCl_3$ lies off the linear relationship of $V_A/V_B \sim \Phi$. There is also a large Δ_{perp} value, defined as $\Delta_{perp} = 1 - \sin\alpha_{xy}\sin\alpha_{yz}\sin\alpha_{zx}$, where α_{xy} is the angle between the two stalks closest to the *x*- and *y*- axis respectively. Δ_{perp} for most perovskites is an order of less 10^{-3}, in the list of Thomas [36], with the exception of $NaTaO_3$, Rb_3PdD_3 and $MAPbBr_3$ [6,36].

Table 5 shows lattice parameters refined from some rapid scans as a function of temperature for data refined in *Pnma.* The corresponding spontaneous strains e_1, e_2, e_3 are shown in Fig. 4. Here $e_1 = (a - a_0)/a_0(T)$, *a* is the lattice parameter of *Pnma* and $a_0(T)$ that extrapolated from the cubic parent cell. e_2 and e_3 are similarly defined with respect to the *b* and *c* axes. The results suggest that *a* and *b* strain to keep *c* close to that which one would expect from the cubic parent cell, since e_3 is close to zero

Table 2
Refined atomic coordinates and thermal parameters in the ordered phase of $MAPbCl_3$ at 80 K

Name	X	Y	Z	U_i* 100 (Å^2)	Site symmetry
PB1	0.24364(11)	0.50160(17)	0.22515(7)	0.351(28)	1
CL2	0.2208(8)	0.250000	0.2193(6)	0.88(16)	M(010)
CL3	0.2809(5)	0.4725(4)	0.4720(4)	1.44(11)	1
CL4	−0.0154(4)	0.4683(4)	0.2951(4)	1.56(12)	1
CL5	0.2787(8)	0.750000	0.2220(6)	0.94(17)	M(010)
C6	0.5197(7)	0.250000	0.5452(5)	1.57(10)	M(010)
N7	0.4616(5)	0.250000	0.4274(4)	1.57(10)	M(010)
H8	0.4519(11)	0.250000	0.6135(4)	5.43(16)	M(010)
H9	0.5748(8)	0.172340	0.5541(7)	5.43(16)	1
H10	0.5748(8)	0.327660	0.5541(7)	5.43(16)	1
D11	0.5262(6)	0.250000	0.3623(5)	5.43(16)	M(010)
D12	0.4091(5)	0.324064	0.4189(5)	5.43(16)	1
D13	0.4091(5)	0.175936	0.4189(5)	5.43(16)	1
C14	−0.0585(5)	0.250000	0.5409(7)	1.57(10)	M(010)
N15	0.0559(4)	0.250000	0.4748(5)	1.57(10)	M(010)
H16	−0.1322(4)	0.250000	0.4789(11)	5.43(16)	M(010)
H17	−0.0634(7)	0.172340	0.5959(7)	5.43(16)	1
H18	−0.0634(7)	0.327660	0.5959(7)	5.43(16)	1
D19	0.1262(5)	0.250000	0.5339(7)	5.43(16)	M(010)
D20	0.0606(5)	0.324064	0.4223(5)	5.43(16)	1
D21	0.0606(5)	0.175936	0.4223(5)	5.43(16)	1

Table 3
Selected bond lengths (Å) and angles (°) in $PbCl_6$ octahedron and $MACl_{12}$ cage for $MAPbCl_3$ at 80 K

Internal	$PbCl_6$ octahedron	$MACl_{12}$ cage	
PB1_CL2	2.8691(20)	H8_Cl5	2.85(1)
PB1_CL3	2.835(5)	H9,10_Cl3	2.800(8)
PB1_CL3	2.884(5)	D11_Cl2	2.36(1)
PB1_CL4	3.024(5)	D12,13_Cl3	2.292(6)
PB1_CL4	2.729(5)	H16_Cl2	2.77(1)
PB1_CL5	2.8480(22)	H17,18_Cl4	2.767(8)
		D19_Cl5	2.374(9)
CL2_PB1_CL3	85.39(16)	D20,21_Cl4	2.337(6)
CL2_PB1_CL3	94.03(15)		
CL2_PB1_CL4	78.26(20)	C6_H8…Cl5	159.9(4)
CL2_PB1_CL4	87.00(21)	C6_H9,10…Cl3	168.6(3)
CL2_PB1_CL5	176.52(28)	N7_D11…Cl2	157.4(5)
CL3_PB1_CL3	176.88(6)	N7_D12,13…Cl3	158.8(3)
CL3_PB1_CL4	82.51(15)	C14_H16…Cl2	166.6(5)
CL3_PB1_CL4	85.48(16)	C14_H17,18…Cl4	157.4(3)
CL3_PB1_CL5	96.17(16)	N15_D19… Cl5	156.9(5)
CL3_PB1_CL4	100.38(15)	N15_D20,21…Cl4	155.1(3)
CL3_PB1_CL4	91.44(16)		
CL3_PB1_CL5	84.24(16)	Pb–Cl–Pb angles	
CL4_PB1_CL4	161.64(17)	PB1_CL2_PB1	169.47(33)
CL4_PB1_CL5	105.01(21)	PB1_CL3_PB1	161.24(18)
CL4_PB1_CL5	90.02(21)	PB1_CL4_PB1	154.89(19)
		PB1_CL5_PB1	164.1(4)

for all temperatures. We also note in passing that we appear to have caught near 170 K, Phase II, the incommensurately modulated structure based around a tetragonal precursor. In this structure we find that *a* and *b* become nearly equal, so that the *c*-axis of the *Pnma* structure, likely corresponds to the quasi-tetragonal axis of Phase II. Below 170 K, the strain significantly increases along [100], probably related to the alternating long and short Pb–Cl bond lengths in this direction.

3.1. Comparison to other organic–inorganic lead halides perovskites

$MAPbBr_3$ has been shown to order in the space group *Pnma*, consistent with the standard $a^-b^+a^-$ tilt system, resulting in a relationship of ($\sqrt{2}a_p$, $2a_p$, $\sqrt{2}a_p$) with respect to the cubic phase. It also seems that $MAPbI_3$ possesses the same structure as $MAPbBr_3$ [4,6].

The distortion of the $PbBr_6$ octahedron in the ordered phase of $MAPbBr_3$ was shown to be quite considerable, when compared to the many other perovskites in the standard *Pnma* tilt system, whereas the refined geometry of the MA ion showed little distortion from an ideal *trans* configuration [12]. This strongly suggested that the more rigid of the two molecular ions is the cation, and not the anion. When considering crystal chemistry on going from $MAPbBr_3$ to $MAPbCl_3$, there are two competing effects with regards to the distortions of the octahedra. Shorter bond lengths of octahedra usually correspond to higher bond strengths, and one might therefore expect a relatively more rigid octahedron. However, shrinking the octahedra also shrinks the cage containing the MA ion, and the D…X hydrogen bond strength also increases. A comparison is given in Table 4. The function Φ, which represents total tilting of the system, is smaller in $MAPbCl_3$ than $MAPbBr_3$. Table 4 shows that the distortion of the individual octahedra of

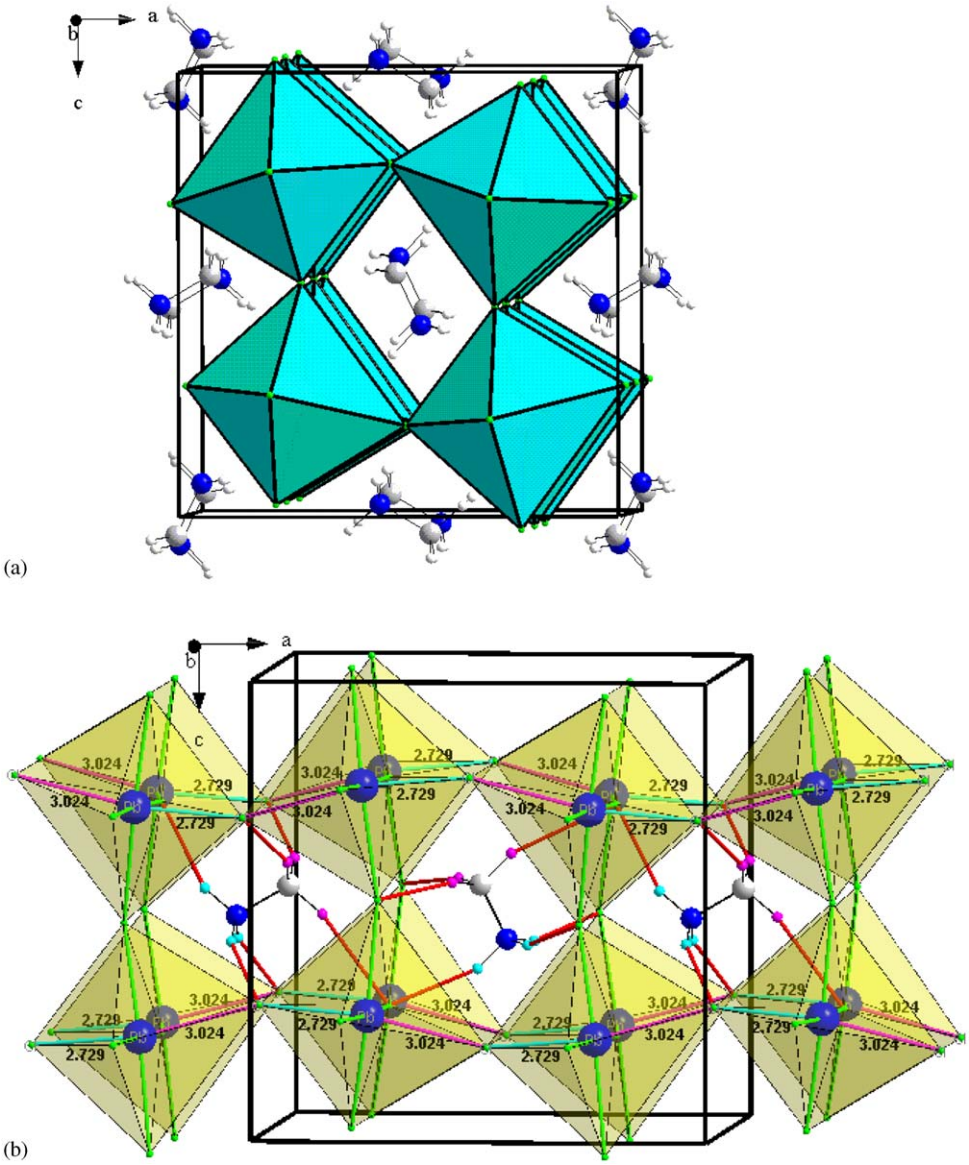

Fig. 3. (a) View of the ordered phase of methylammonium lead chloride along *b*. Two MA cations reside in the *ac* plane. (b) Connectivity between $PbCl_6$ octahedra and MA cation, showing alternately long and short Pb-Cl bond lengths along *a* while one hydrogen bonds a shared chloride atoms and two hydrogen bond to two chlorine atoms respectively.

Table 4
Calculated polyhedral distortion parameters defined by Thomas [35] for $MAPbCl_3$ and $MAPbBr_3$ [6]

$MAPbCl_3$							
θ_m	4.695°	V_B	30.572 Å	$V_{A,1}$	155.799 Å^3	$V_{A,1}/V_B^a$	5.096
θ_z	7.89°	QE_B	1.018	$V_{A,2}$	149.391 Å^3	$V_{A,2}/V_B^a$	4.887
Φ	1.61×10^{-2}	BAV_B	60.663°^{2}	V_A/V_B^t	4.903	$\Delta V_{A,1}/V_B$	−0.193
Δ_{perp}	1.283×10^{-2} Å	$(S_1+S_2)^2/S_1S_2$	4.000			$\Delta V_{A,2}/V_B$	0.016
$MAPbBr_3$							
θ_m	11.352°	V_B	34.9556 Å	V_A	167.226Å^3		
θ_z	5.862°	QE_B	1.00738	V_A/V_B^a	4.784		
Φ	4.38×10^{-2}	BAV_B	26.502°^{2}	V_A/V_B^t	4.737		
Δ_{perp}	1.107×10^{-2} Å	$(S_1+S_2)^2/S_1S_2$	4.000	$\Delta V_A/V_B$	−0.047		

Table 5
The lattice parameters of $MAPbCl_3$ at different temperatures. Over 190 K, $MAPbCl_3$ was refined in $Pm\bar{3}m$

T (K)	a (Å)	b (Å)	c (Å)
3.5	11.157(1)	11.349(1)	11.275(2)
40	11.146(2)	11.338(2)	11.263(2)
80	11.164(1)	11.349(1)	11.278(1)
95	11.163(1)	11.345(1)	11.292(1)
110	11.165(3)	11.345(3)	11.275(3)
150	11.187(3)	11.343(3)	11.282(3)
160	11.193(3)	11.347(3)	11.287(3)
170	11.331(2)	11.318(2)	11.290(2)
190	5.656(2)		
220	5.659(2)		
250	5.664(2)		
280	5.669(4)		

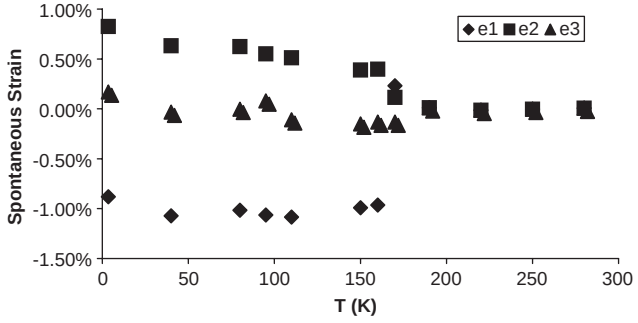

Fig. 4. Temperature dependence of spontaneous strain e_1, e_2 and e_3 in phases I and III.

$MAPbCl_3$ exceeds those of $MAPbBr_3$. This is shown by the values of the quadratic elongation, QE_B, and bond angle variance, BAV_B , calculated using VOLCAL [39]. This observation across the halides implies that the relative rigidity of the MA cation exceeds that of the octahedra in these salts. This observation agrees with the mode assignments of Raman spectra, in which the Raman-active internal modes of the distortions of the octahedron are all less than $\sim 320\,cm^{-1}$, whereas the Raman-active internal modes of the MA cation are all $\sim 480\,cm^{-1}$ and above [23,24].

The behavior shown in the methylammonium lead halide true perovskites contrasts with the distortions seen in certain lead halide layered perovskites. Calculations on the geometry of the octahedra in phenethylammonium (PE) lead chloride $(C_6H_5C_2H_4NH_3)_2PbCl_4$ [40] using IVTON and VOLCAL [37–39] show that the off-centroid displacement of the two Pb atoms in the lead chloride octahedra are similar at 0.173 and 0.175 Å. This compares to a slightly smaller value in $MAPbCl_3$ of 0.145 Å. The volumes and quadratic elongations of the two octahedra in the PE-salt are essentially identical at 31.8 $Å^3$ and 1.006, respectively, and they possess similar bond angle variances of 18.2 and 18.7 $°^2$. This is significantly smaller than the 60.6 $°^2$ for $MAPbCl_3$ (Table 4).

We note that in $(C_6H_5C_2H_4NH_3)_2PbCl_4$ the PE-cation is in an unusual *J*-shaped conformation, in which the terminal amine is curved back over the phenyl ring, as opposed to what is expected to be the most stable *trans*-configuration of the chain [40]. This implies the energy penalty for this conformational change of the PE chain must be comparable to those for distortions of the octahedra. A comparable soft conformational change is not possible for MA. It is likely that the additional internal deformation of the octahedra in $MAPbCl_3$ comes from having to close the 3*d*-framework around the relatively rigid MA ion.

3.2. Symmetry analysis

The *Pnma* space group with basis $(2a_p, 2a_p, 2a_p)$, where a_p is the lattice of the parent $Pm\bar{3}m$ cell, does not conform to a space group expected from a pure tilt transition with a simple cation [8]. The group–subgroup relationship is shown in Fig. 5, with the matrices relating group to subgroup cells. This analysis was performed with the package ISOBYU [41]. The point symmetry and relationship between the Wyckoff sites of Pb and MA are also shown. It appears that the cell is most closely related to the *Cmcm* space group associated with the $a^0b^+c^-$ standard tilt system; both the cell basis and the site symmetries of the octahedra and MA ion map as one would expect if this were the case.

It is clear that the MA cations could not order in *Cmcm* (Fig. 5) as the *A*-site symmetry is not compatible with such a state. However, it is also clear that it is not just the orientational ordering of the MA ions that break the symmetry. The large internal distortions of the octahedra from centrosymmetry are revealed by the bond lengths in Table 3. The Pb atom is approximately 0.29 Å from the (1/4, 1/2, 1/4) position it would inherit from a hypothetical *Cmcm* structure.

4. Conclusions

$MAPbCl_3$ orders in the centrosymmetric space group *Pnma*, but with $(2a_p, 2a_p, 2a_p)$ basis rather than the $(\sqrt{2}a_p, 2a_p, \sqrt{2}a_p)$ basis usually associated with perovskites in this space group. It is therefore not related to $GdFeO_3$ structure. $MAPbCl_3$ does not occupy a structure that can be generated solely via the classical tilt instabilities. We have previously shown that $MAPbBr_3$ (and therefore $MAPbI_3$) is also centrosymmetric. Therefore, contrary to the original suggestions of Poglitsch and Weber [4], the $MAPbX_3$ are not ferroelectrics in their ordered states.

The $MAPbX_3$ can be viewed as a "molecular structure" formed of concatenated molecular anions and isolated molecular cations. Due to the concatenation, it may not be possible for both the anions to

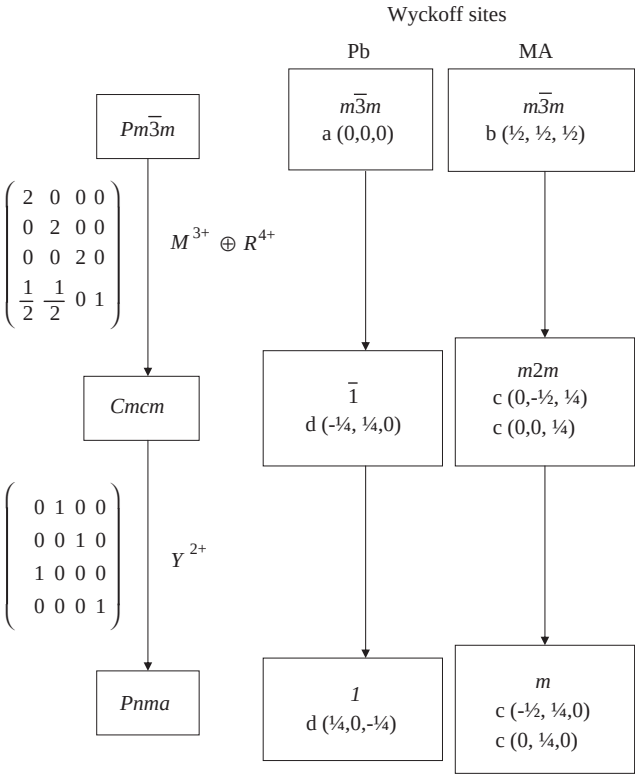

Fig. 5. Group–subgroup relationship between the cubic aristotype $Pm\bar{3}m$, the standard *Cmcm* $a^0b^+c^-$ space group associated with the tilt system ABC, and the *Pnma* cell found for the ordered phase of methylammonium lead chloride. The matrices contain the origin shift and relate the basis of the new cell to that of the parent cell.

undergo pure tilting and the cations to orientationally order; distortion of one or the other may be necessary. The more compliant of these two groups would deform in preference to the other. Shrinking the octahedral size also shrinks the cage for the MA cations, and this is coupled to more, rather than less, distortion of the octahedra. This implies that MA is the more rigid of the two molecular ions. This has potential implications for the behavior of these salts under pressure. It also provides an example of the limitation of the approximation of rigid octahedra for the prediction of tilt-related structural transitions in perovskites.

These observations demonstrate that one has to consider the order–disorder phenomena of the MA cations and the framework as a coupled system. In the case of $MAPbBr_3$ the structure can be rationalized as being, to first order, a framework-driven tilt instability, in which deformation of octahedra are not required, but are allowed. These secondary distortions of the octahedra in $MAPbBr_3$ are in fact quite large [6]. In $MAPbCl_3$, MA is not a "passive" cation stabilizing a tilt system. Our symmetry analysis suggests that the *Pnma* cell, in which the MA ions are ordered, is a subgroup of the *Cmcm* tilt system. The size of the distortion of the octahedra is substantial. This suggests that for $MAPbX_3$ the RUMs and certain distortional modes of the octahedra lie on a similar energy scale. This may be because, compared to most other perovskites [36], the octahedra are relatively large, and hence intrinsically less rigid.

References

[1] R.H. Mitchell, Perovskites: Modern and Ancient, Almaz Press, Thunder Bay, ON, 2002.
[2] J. Rubin, E. Palacios, J. Bartolomé', J. Rodriguez-Caravajal, J. Phys. Condens. Matter 7 (1995) 563–575.
[3] D. Weber, Z. Naturforsch. 33B (1978) 1443–1445.
[4] A. Poglitch, D. Weber, J. Chem. Phys. 87 (1987) 6373–6378.
[5] O. Knop, R.E. Wasylishen, M.A. White, T.S. Cameron, M.J.M. Van Oort, Can. J. Chem. 68 (1990) 412–422.
[6] I.P. Swainson, R.P. Hammond, C. Soullière, O. Knop, W. Massa, J. Solid State Chem. 176 (2003) 97–104.
[7] D.B. Mitzi, K. Liang, J. Solid State Chem. 134 (1997) 376–381.
[8] Y. Lee, D.B. Mitzi, P.W. Barnes, T. Vogt, Phys. Rev. B 68 (2003) 020103-1–020103-4.
[9] G. Dolling, B.M. Powell, V.F. Sears, Mol. Phys. 37 (1979) 1859–1883.
[10] A.P. Giddy, M.T. Dove, G.S. Pawley, V. Heine, Acta Crystallogr. A 49 (1993) 697–703.
[11] K.D. Hammonds, A. Bosenick, M.T. Dove, V. Heine, Am. Mineral. 83 (1998) 476–479.
[12] A.M. Glazer, Acta Crystallogr. B 28 (1972) 3384–3392.
[13] A.M. Glazer, Acta Crystallogr. A 31 (1975) 756–762.
[14] C.J. Howard, H.T. Stokes, Acta Crystllogr. B 54 (1998) 782–789.
[15] G. Hua, J. Phys. Condens. Matter 3 (1991) 1371–1388.
[16] Y. Fujii, S. Hoshino, Y. Yamada, G. Shirane, Phys. Rev. B 9 (1974) 4549–4559.
[17] D.B. Mitzi, C.A. Field, Z. Schlesinger, R.B. Laibowitz, J. Solid State Chem. 114 (1995) 159–163.
[18] D.B. Mitzi, S. Wang, C.A. Field, C.A. Chess, A.M. Guloy, Science 267 (1995) 1473–1476.
[19] K. Yamada, K. Mikawa, T. Okuda, K. Knight, J. Chem. Soc. Dalton Trans. (2002) 2112–2118.
[20] K. Yamada, K. Isobe, T. Okuda, Y. Furukawa, Z. Naturforsch. A 49 (1994) 258.
[21] R.E. Wasylishen, O. Knop, J.B. Macdonald, Solid State Commun. 56 (1985) 581–582.
[22] A. Maalej, Y. Abid, A. Kallel, A. Daoud, A. Lautié, F. Romain, Solid State Commun. 103 (1997) 279–284.
[23] A. Maalej, M. Bahri, Y. Abid, N. Jaïdane, Can. J. Phys. 77 (1999) 717–722.
[24] A. Maalej, M. Bahri, Y. Abid, N. Jaïdane, Z.B. Lakhdar, A. Lautié, Phase Trans. 64 (1998) 179–190.
[25] N. Onoda-Yamamuro, T. Matsuo, H. Suga, J. Phys. Chem. Solids 51 (1990) 1383–1395.
[26] A. Maalej, Y. Abid, A. Kallel, A. Daoud, A. Lautié, Ann. Chim. Sci. Mat. 23 (1998) 241–246.
[27] Y. Kawamura, H. Mashiyama, J. Korean Phys. Soc. 35 (1999) S1437–S1440.
[28] R. Shirley, CRYSFIRE Suite, The Lattice Press 41, Guildford Park Avenue, Guildford, Surrey, UK, 1999.
[29] A. Altomare, M.C. Burla, M. Camalli, B. Carrozzini, C.L. Cascarano, C. Giacovazzo, A. Guagliardi, A.G.G. Moliterni, G. Polidori, R. Rizzi, J. Appl. Cryst. 26 (1993) 343–350.
[30] V. Favre-Nicolin, R. Cern, J. Appl. Cryst. 35 (2002) 734–743.
[31] A. Larson, R. Vondreele, GSAS: General Structure Analysis System, LAUR 86–748, Los Alamos, NM, 1986.

[32] A.L. Spek, PLATON—A Multi-Purpose Crystallographic Tool, Utrecht University, The Netherlands, 1999.
[33] E.J. MacLean, K.D.M. Harris, B.M. Kariuki, S.J. Kitchin, R.R. Tykwinski, I.P. Swainson, J.D. Dunitz, J. Am. Chem. Soc. 125 (2003) 14449–14451.
[34] I.P. Swainson, M.T. Dove, Am. Mineral. 22 (1995) 61–65.
[35] V. Heine, P.R.L. Welche, M.T. Dove, J. Am. Ceram. Soc. 82 (1999) 1793–1802.
[36] N.W. Thomas, Acta Cryst. B 52 (1996) 16–31.
[37] T. Balić Žunić, I. Vicković, J. Appl. Crystallogr. 29 (1996) 305–306.
[38] L. Farrugia, J. Appl. Cryst. 32 (1999) 837–838.
[39] L.W. Finger, VOLCAL, Carnegie Institute of Washington, Geophysical Laboratory, Washington, DC, 1971.
[40] D.B. Mitzi, J. Solid State Chem. 145 (1999) 694–704.
[41] H.T. Stokes, D.M. Hatch, ISOTROPY. Version 6.4.2. http://stokes.byu.edu/isotropy.html, Department of Physics, Brigham Young University, UT, 2002.